AAS 24-174

ORION ARTEMIS I ENTRY PERFORMANCE

Jeremy Rea* **and Luke McNamara†** **and Mark Kane‡**

The Artemis I mission successfully demonstrated the Orion Multi-Purpose Crew Module ability to perform a skip re-entry with predictive guidance to reach the target splashdown location. Skip re-entry improves the down-range capability for precision landing, allowing Orion to return to the continental United States at any time during the lunar month, and improves the survivability from a wide range of return trajectories. This paper presents analysis of Orion skip re-entry Guidance and Control performance for the Artemis I mission utilizing recorded flight data and high fidelity simulation data. Descriptions of the related Guidance and Control designs are provided for understanding.

INTRODUCTION

The NASA Orion Artemis I mission launched on November 16, 2022 at 1:47 a.m. EST from the NASA Kennedy Space Center using the newly designed NASA Space Launch System (SLS). This was the last planned uncrewed Artemis mission prior to flying the Artemis II crewed mission using the Orion spacecraft and the SLS. It followed NASA flight tests Ares I-X (2009), Pad Abort 1 (2010), Exploration Flight Test 1 (2014), and Ascent Abort 2 Flight Test (2019). The uncrewed Artemis I mission was a lunar flight test that successfully stressed Orion's systems and completed many Flight Test Objectives to prepare Orion for future missions. It was the first in a series of increasingly complex missions that will enable human exploration at the Moon.

The Artemis I mission duration of 25 days, 10 hours and 53 minutes included 6 days spent in a Distant Retrograde Orbit (DRO). Orion flew as close as 80 miles[1] from the lunar surface. After the DRO the spacecraft returned to Earth and re-entered the atmosphere at approximately 11 $\frac{km}{sec}$ (36,090 $\frac{ft}{sec}$). Once inside the atmosphere, the vehicle flew a guided entry using bank angle modulation. The vehicle targeted a splashdown location in the Pacific Ocean, southwest of San Diego, CA.

The Guidance, Navigation, and Control (GN&C) system worked successfully to enable the completion of mission objectives including skip entry amongst many others. The entry trajectory's bank modulation was commanded by the entry Flight Software (FSW). Specifically, the guidance algorithm PredGuid[2–5] used a numeric predictor corrector (NPC) paired with the flight-tested Apollo Final Phase guidance algorithm[6] to perform a skip entry and target the desired landing site.

ENTRY SEQUENCE

The entry sequence began at the separation of the Crew Module (CM) from the Service Module (SM) prior to the Entry Interface (EI) illustrated in Figure 1(a). Immediately after CM-SM separation the CM vehicle inhibited RCS firings to protect against recontact with the SM. Then it performed a closed-loop exo-atmospheric CM Raise Burn (also known as CM Translation Burn) to shallow the predicted EI flight path angle to the EI target, and to ensure effective SM debris disposal. Next the vehicle was rotated to heatshield

*Orion Entry GN&C MODE Team Guidance Sub-System Manager and Guidance Technical Discipline Lead, Flight Mechanics & Trajectory Design Branch, NASA Johnson Space Center, Houston, Texas, 77058, USA.
†Orion Entry GN&C MODE Team Member, Flight Mechanics & Trajectory Design Branch, NASA Johnson Space Center, Houston, Texas, 77058, USA.
‡Orion Entry GN&C MODE Team Lead and System Manger, Integrated GN&C Analysis Branch, NASA Johnson Space Center, Houston, Texas, 77058, USA.

forward to prepare for entry. EI was targeted above the southern Pacific Ocean. Due to weather, a landing site off the western coast of Baja California was selected roughly 300 miles south of the primary landing zone. Figure 2 shows the Artemis I trajectory from EI to splashdown relative to the EI Target Line and the allowable EI zone for proper SM disposal.[7] Table 1 gives the EI state position and velocity elements. Note that the EI geodetic altitude for Earth was defined as 400 kft and represents a convenient point to consider the impacts of the atmospheric density on the vehicle. During the hypersonic, supersonic, and subsonic portion of the trajectory the vehicle was banked by guidance pointing the vehicle's lift vector in order to target the designated landing site. During the Landing and Recovery System (LRS) sequence, the CM deployed the Forward Bay Cover (FBC) pilot parachutes pulling away the FBC, deployed two drogue parachutes, released the drogue parachutes, and deployed three pilot parachutes that pulled out the three main parachutes. The described parachute sequence for the Artemis I Entry, Descent & Landing flight is illustrated in Figure 1(b).

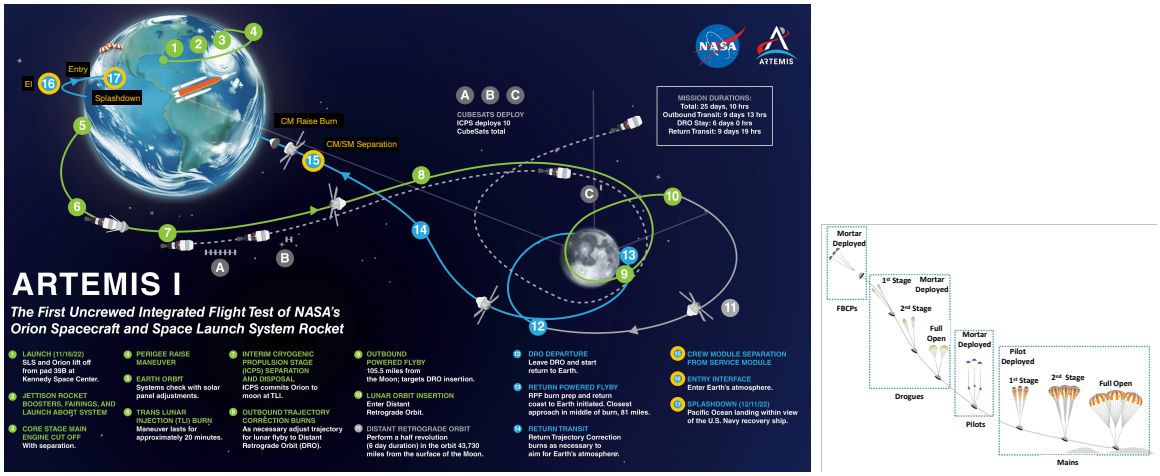

(a) Overall Mission Sequence[8]

(b) Parachute Sequence[9]

Figure 1: Orion Artemis I: Nominal Sequences

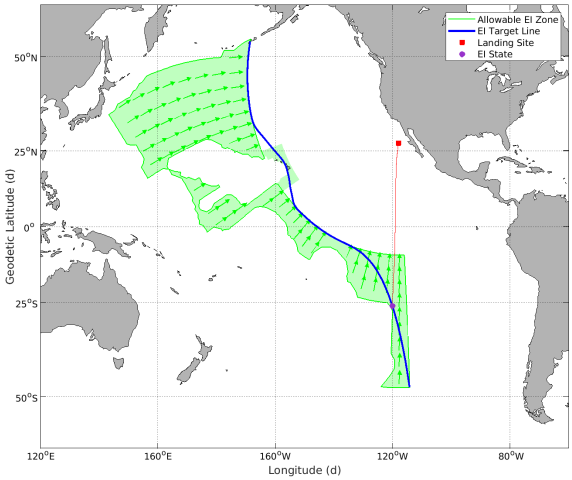

Figure 2: Artemis I Trajectory from EI to Splashdown

Table 1: Artemis I Entry Interface State

Parameter	Units	Artemis I
Geodetic Altitude	ft	400000.0
Geodetic Latitude	deg	-25.82847
Longitude	deg	-120.08071
Inertial Velocity Magnitude	ft/s	36062.65680
Inertial Topocentric Flight Path Angle	deg	-5.66367
Inertial Topocentric Azimuth	deg	4.65389
Total Range-to-Target	nmi	3176.65
Lateral Angle	deg	0.94018

ENTRY GUIDANCE

In the following sections, comparison plots will be shown between Artemis I flight parameters (labeled "Artemis I"), the best simulated prediction of the flight (labeled "Predicted"), and the expected dispersion

envelope (labeled "Dispersed").

Guidance Design and Methodology

The PredGuid entry guidance algorithm generates a bank command to guide the vehicle from EI through the atmosphere to a target site while meeting constraints on heating, g-load, and fuel usage. The downrange between EI and the target site can vary broadly with incoming orbit geometry, and the vehicle experiences dispersed conditions in atmosphere, aerodynamic properties, and EI conditions. PredGuid builds on the heritage of Apollo's entry guidance algorithm, making alterations only where necessary to improve performance. Apollo included a skip entry capability, but it was never flown and was considered a backup capability. Various structural and aeroheating design constraints have resulted in a lower L/D for Orion than Apollo, and therefore lower control authority. Several enhancements to the Apollo algorithm were necessary to meet Orion requirements and make the skip entry robust for nominal operations:

1. A Numerical Predictor-Corrector (NPC) for range prediction, rather than analytic methods, in early entry guidance phases
2. In-flight estimation of atmospheric density and vehicle L/D variations
3. Interpolation of the Final phase reference trajectory, rather than nearest-neighbor
4. The addition of Terminal phase steering

These algorithm elements work together to provide significant long-range skip entry performance benefits over the original Apollo algorithm. The replacement of the Apollo analytic range estimates with the NPC algorithm during several entry phases accounts for a large part of the improvement. For this, PredGuid incorporates a modified version of the PRED GUID NPC algorithm, originally developed for the Aeroassist Flight Experiment (AFE), into the Apollo entry guidance[4,10]. The NPC uses a unique corrector method to find a solution to the constant bank angle trajectory problem. First, the predictor is used to numerically propagate a constant bank angle trajectory from the current vehicle state to the appropriate Final phase conditions at second entry. If the calculated range over this propagation is within a given tolerance, the constant bank angle used to generate the trajectory is output to flight control. If the range is not within the tolerance, the corrector determines a new bank angle and the predictor is run again. The resulting bank angle accurately guides the vehicle to the Final phase initial condition. PredGuid performs closed-loop updates to the bank angle each guidance cycle using the current best knowledge of L/D, atmospheric density, and range.

The PredGuid entry guidance has 6 phases as shown in Figure 3. Figure 3(a) shows the PredGuid phases in parallel, where the path through the figure is determined by the current phase. The figure reflects how PredGuid decouples longitudinal flight, which controls downrange, from lateral flight, which controls crossrange, until the Terminal phase, where corrections in the downrange and crossrange channels are coupled. Figure 3(b) and Table 2 show the predicted and actual phase transitions for the Artemis I entry in the space of geodetic altitude versus range. The expected range of dispersed flight is also shown. Each phase will be discussed in more detail in the following sections with performance comparisons between the Artemis I flight and the best simulated prediction.

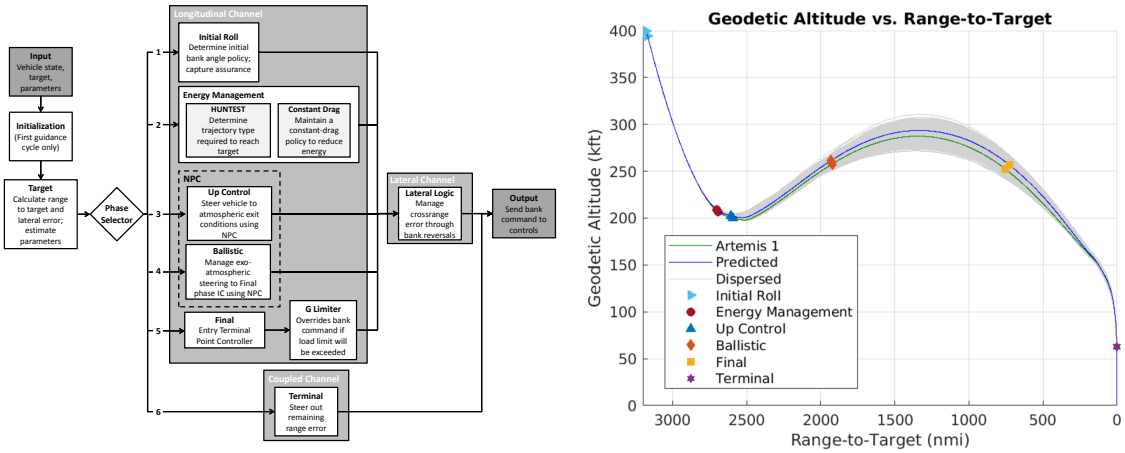

(a) PredGuid Algorithm Phases Diagram

(b) PredGuid Artemis I Phase Transitions

Figure 3: PredGuid Entry Guidance Phases

Table 2: PredGuid Actual and Predicted Phase Transition Timing

Phase Initiation/Event	**Time Relative to EI (s) Artemis I**	**Time Relative to EI (s) Predicted**
PredGuid Initial Roll	1.475	3.00
PredGuid Energy Management	83.475	82.00
PredGuid Up Control	102.475	100.00
PredGuid Ballistic	256.450	255.00
PredGuid Final	551.425	560.00
PredGuid Terminal	882.400	877.00
FBC Pilot Chute Deploy	950.125	946.15

PredGuid Phase 1: Initial Roll This phase holds a pre-selected bank angle, but switches command to lift-down if the vehicle is above a parameterized skip out boundary threshold when a parameterized drag threshold is first reached. For Artemis I, the vehicle hit the desired EI target and did not trigger the skip out protection logic. The pre-selected bank angle command was 0°, however PredGuid preserves lateral capability by limiting the bank command to 15°. The Initial Roll phase ends when the altitude rate goes above -700 ft/s. Figure 4(a) shows the bank command during the Initial Roll phase. Figure 4(b) shows the altitude rate. The actual flight and predicted bank commands during this phase agree, with only slight variations in the transition into and out of the phase. The transition to the Energy Management phase occurs as expected.

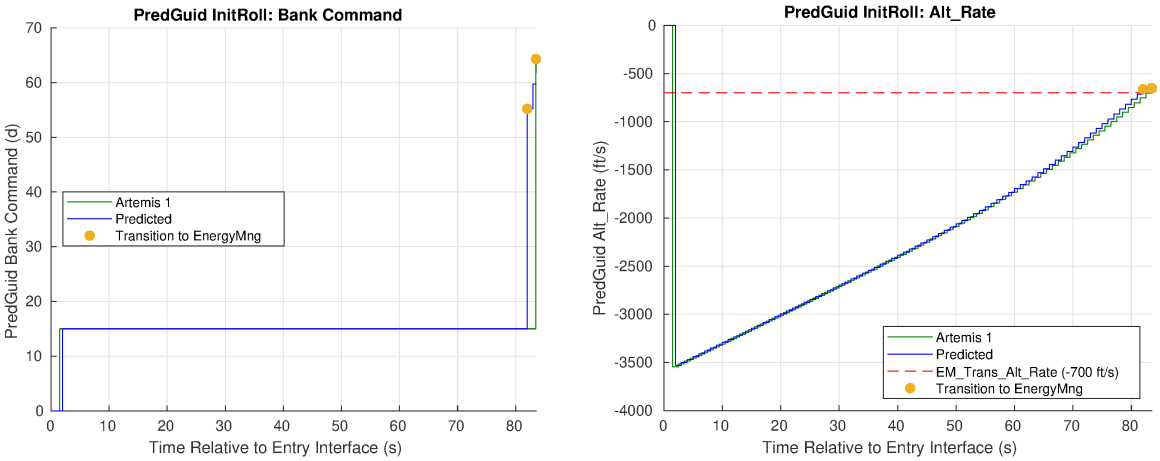

(a) Artemis I PredGuid InitRoll Phase: Bank Command vs. Time (b) Artemis I PredGuid InitRoll Phase: Altitude Rate vs. Time

Figure 4: Artemis I PredGuid InitRoll Phase

PredGuid Phase 2: Energy Management This phase retains the original Apollo formulation.[6] There are two sub-phases: Huntest and Constant Drag. Huntest hunts for an estimate of the initial velocity for the next entry phase that will bring the total range miss below a parameterized tolerance using an analytic predictor-corrector, assuming a constant vertical L/D between Up Control and Final. Constant Drag selects the constant vertical L/D command to reach that velocity by the start of the next phase. The Energy Management phase ends when the Huntest range error (Range_Diff) goes below the Range_Tol parameter (40 nmi).

Figure 5(a) shows the bank command during the Energy Management phase. Figure 5(b) shows the Huntest range error (Range_Diff). The differences between the predicted and actual trajectories are due to differences between the predicted and actual atmospheric density encountered during flight. The actual flight and predicted bank commands during this phase agree quite well with about a 1 second difference in the transition time to the Up Control phase.

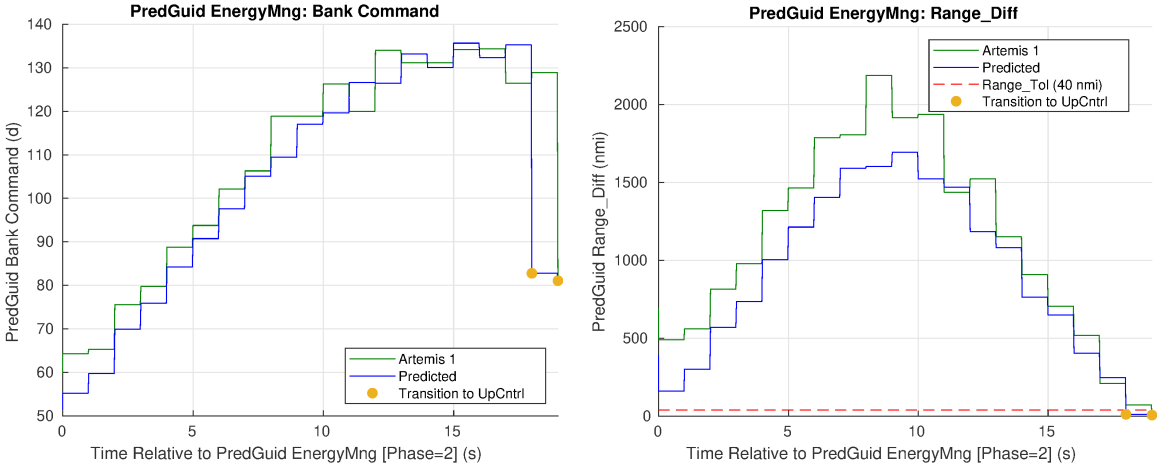

(a) Artemis I PredGuid EnergyMng Phase: Bank Command vs. Time (b) Artemis I PredGuid EnergyMng Phase: Range_Diff vs. Time

Figure 5: Artemis I PredGuid EnergyMng Phase

PredGuid Phase 3: Up Control This phase executes the NPC to find a vertical L/D command to achieve the desired range within a parameterized tolerance. The NPC runs closed-loop during Up Control. The

Up Control phase ends when the drag acceleration (D_Mag) drops below the computed transition drag level (D_Upc_End). D_Upc_End is computed by the NPC and has a minimum allowed value defined by the parameter D_Upc_Min (6 ft/s^2). For skip entries, the value of D_Upc_End should be equal to D_Upc_Min. This was the case for Artemis I.

Figure 6(a) shows the bank command during the Up Control phase. The actual flight and predicted bank commands during this phase agree quite well with about a 1 second difference in the transition time to the Ballistic phase. The trajectories begin to diverge toward the end of the phase. In particular, the second bank reversal did not trigger when predicted. The timing of the second bank reversal is sensitive to small perturbations in the EI state, atmospheric density, and vehicle L/D. It occurs in a low drag region of flight when the vehicle is on the way out of the atmosphere. The timing of the second bank reversal is not a critical driver of the performance during the second entry. Overall, it is not unexpected that the timing of the second bank reversal is mis-predicted.

Figure 6(c) shows the NPC iteration count (NPC_Iter). As expected, the first cycle of PredGuid uses the maximum allowed iterations per cycle of 5. The next 6 cycles use 4 iterations, then all following cycles use between 1 to 3 iterations. When the NPC first activates, it requires more iterations to converge to a solution. This is the expected performance. Figure 6(d) shows the range error (NPC_Range_Error). The NPC is converged when the NPC_Range_Error is less than the NPC_Range_Tol parameter (25 nmi). While the predicted flight did not converge on the first cycle, during the actual Artemis I flight the NPC remained converged for the entire Up Control phase.

Figure 6(b) shows the drag acceleration (D_Mag) along with the value of D_Upc_End. The transition to the Ballistic phase occurs as expected.

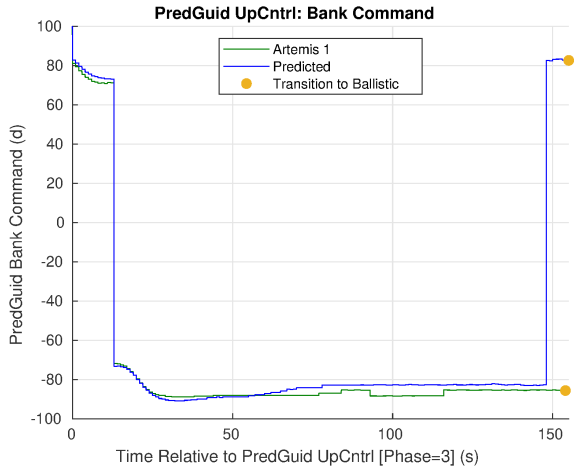

(a) Artemis I PredGuid UpCntrl Phase: Bank Command vs. Time

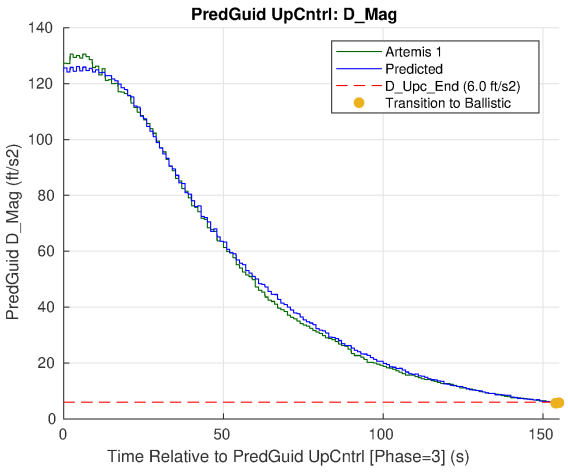

(b) Artemis I PredGuid UpCntrl Phase: D_Mag vs. Time

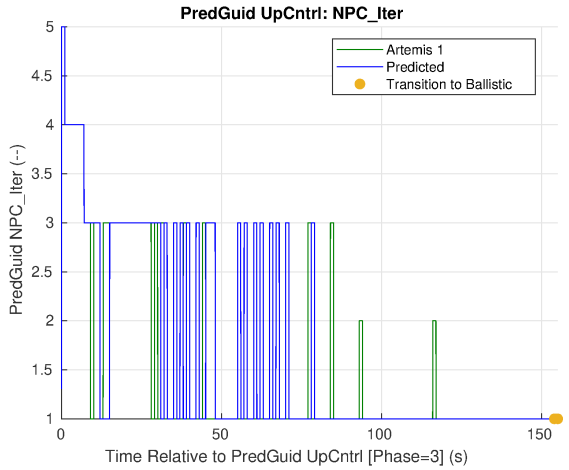

(c) Artemis I PredGuid UpCntrl Phase: NPC_Iter vs. Time

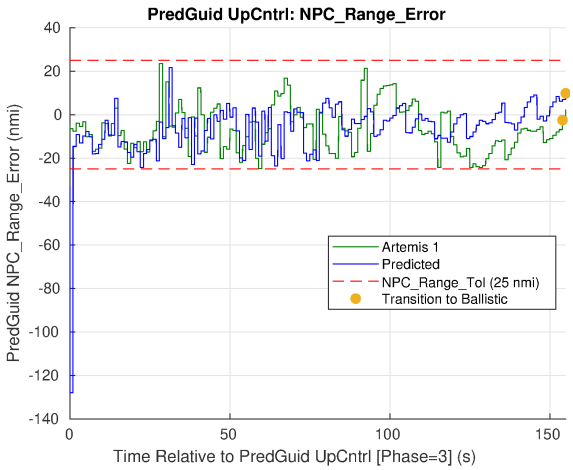

(d) Artemis I PredGuid UpCntrl Phase: NPC_Range_Error vs. Time

Figure 6: Artemis I PredGuid UpCntrl Phase

PredGuid Phase 4: Ballistic This phase corresponds to the exo-atmospheric portion of skip entry and replaces the Apollo Kepler phase. This phase uses the NPC to generate a vertical L/D command in the same way as Up Control. Even with the low control authority during this phase, continuously updating the guidance command results in better performance with minimal increase in fuel usage. Note that the naming of this phase is historical and is not the same as the ballistic spin backup entry guidance. When the predicted range-to-go to the transition to Final phase goes below 100 nmi, the NPC is not called, and the bank angle command is frozen for the remainder of the phase. This is done to avoid numerical instability near the transition. The Ballistic phase terminates when the vehicle re-enters the sensible atmosphere

Figure 7(a) shows the bank command during the Ballistic phase. As discussed in the previous section, the timing of the second bank reversal is different between the actual and predicted trajectories, and so the signs of the actual and predicted bank commands are opposite for much of this phase. Another interesting quirk in the predicted data occurs with a step in the bank command 134 seconds into the phase. This is caused when one cycle of the estimated drag goes above the 1.6 ft/s^2 threshold for the density estimator to activate (see Figure 7(b)). At this point, the density factor is updated, the trajectory prediction is slightly changed, and the bank command to achieve the target also changes. This behavior is not seen in the actual flight data.

Figure 7(c) shows the NPC iteration count (NPC_Iter). As expected, the NPC requires only 1 to 3 iterations to remain converged during the Ballistic phase. Figure 7(d) shows the range error (NPC_Range_Error). The NPC is converged when the NPC_Range_Error is less than the NPC_Range_Tol parameter (25 nmi). The NPC remains converged during the entire Ballistic phase.

Figure 7(b) shows the drag acceleration (D_Mag) along with the values of D_Upc_End and D_Estimators. The transition to the Final phase occurs as expected when the drag acceleration goes above D_Upc_End.

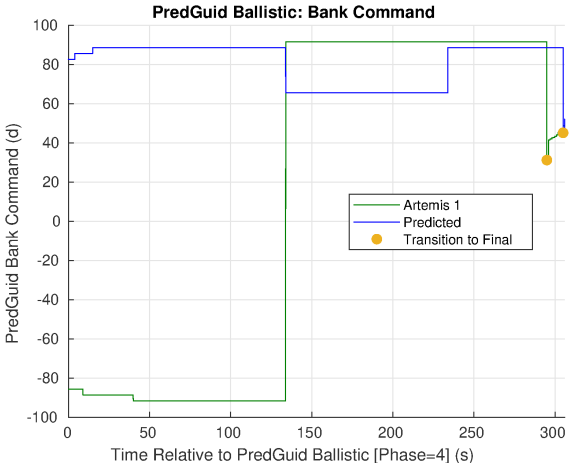

(a) Artemis I PredGuid Ballistic Phase: Bank Command vs. Time

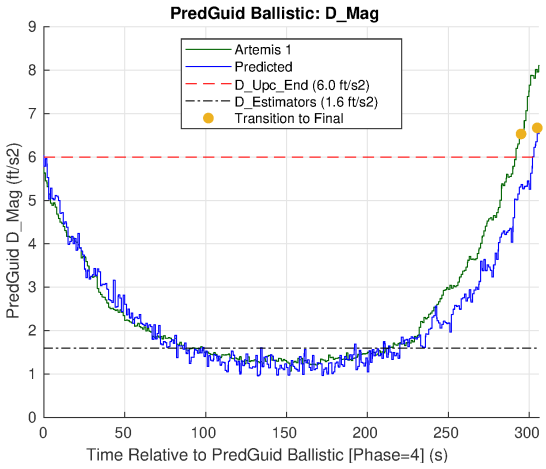

(b) Artemis I PredGuid Ballistic Phase: D_Mag vs. Time

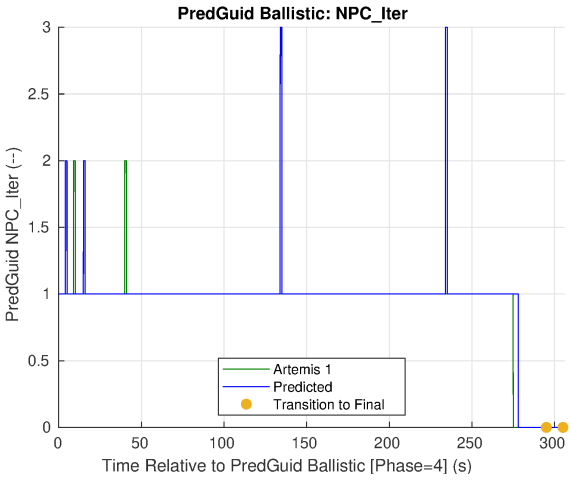

(c) Artemis I PredGuid Ballistic Phase: NPC_Iter vs. Time

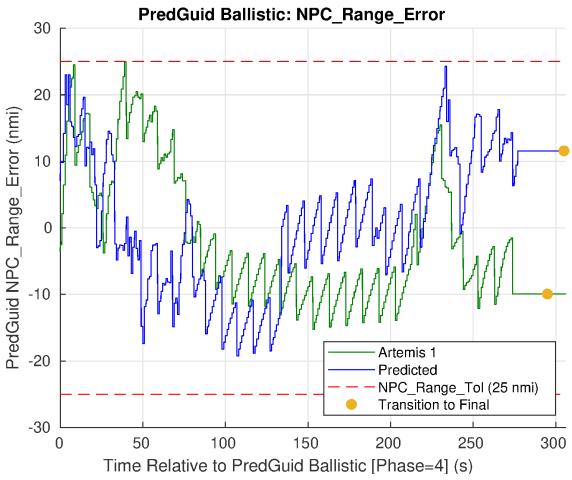

(d) Artemis I PredGuid Ballistic Phase: NPC_Range_Error vs. Time

Figure 7: Artemis I PredGuid Ballistic Phase

PredGuid Phase 5: Final This phase uses an Entry Terminal Point Controller (ETPC) with a stored reference trajectory and gains to determine the desired bank angle. There is also g-limiter logic to alter the bank angle if it detects a possible g-limit violation. During Artemis I, the g-limiter was not activated. The Final phase ends when the speed (V_Mag) drops below the V_Terminal parameter (1000 ft/s).

Figure 8(a) shows the bank command during the Final phase. As discussed in the previous section, the timing of the second bank reversal is different between the actual and predicted trajectories. This change in timing propagates forward into the Final phase and so the timing of all the bank reversals is off between the flight and predicted trajectories.

PredGuid Phase 6: Terminal This phase steers toward the target using a simple proportional guidance scheme based on heading error, freezing the bank command if the vehicle flies past the target. The Terminal phase continues until FBC pilot chute deploy.

Figure 8(b) shows the bank command during the Terminal phase. The actual flight and predicted bank commands during this phase are similar. The differences are due to the actual versus predicted atmosphere and vehicle parameters.

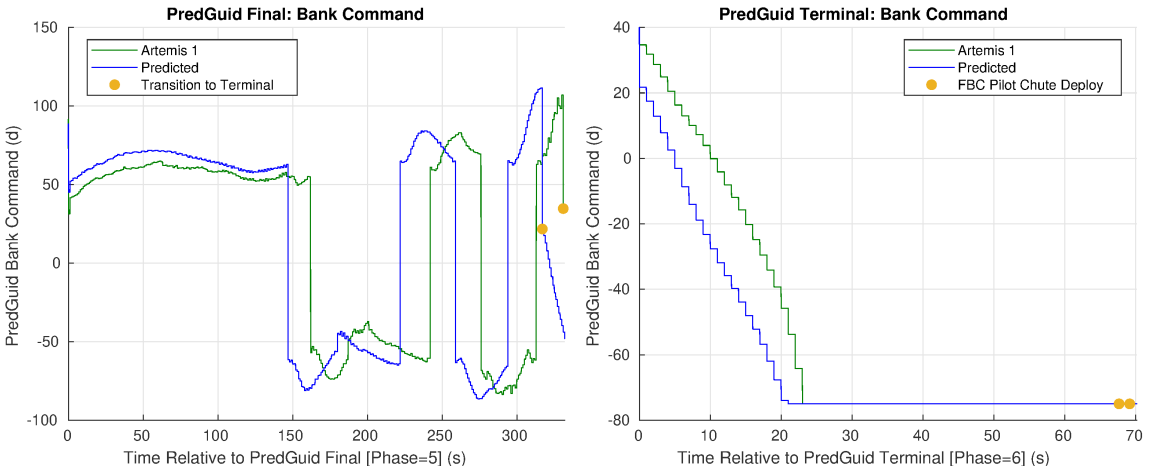

(a) Artemis I PredGuid Final Phase: Bank Command vs. Time (b) Artemis I PredGuid Terminal Phase: Bank Command vs. Time

Figure 8: Artemis I PredGuid Final and Terminal Phase: Bank Command

Lateral Corridor Performance PredGuid uses a decoupled lateral channel to manage crossrange throughout entry. The PredGuid lateral channel guidance is identical to that of the Apollo Lateral Logic, with a modified lateral corridor definition. The lateral channel uses bank reversals to manage crossrange and heading errors. The lateral channel is active from EI until the end of the Final phase. During the Artemis I flight, the entry guidance commanded 6 bank reversals. This matched the predicted number of reversals. Figure 9(a) shows the PredGuid lateral angle (Lat_Ang) and the lateral angle deadband (Lat_Db). Figure 9(b) shows the same data zoomed in near the end of guided flight. Table 3 gives the bank reversal initiation times relative to EI. Differences were seen between the flight and prediction in both the atmospheric density and L/D. The cumulative impact of these differences shifts the timing of the bank reversals, with the changes becoming larger later in the trajectory.

Table 3: Artemis I Bank Reversal Initiation Times

Bank Reversal Initiation	**Time Relative to EI (s) Artemis I**	**Time Relative to EI (s) Predicted**
1	115.475	113.0
2	390.450	248.0
3	713.425	707.0
4	793.425	782.0
5	827.425	819.0
6	864.400	854.0

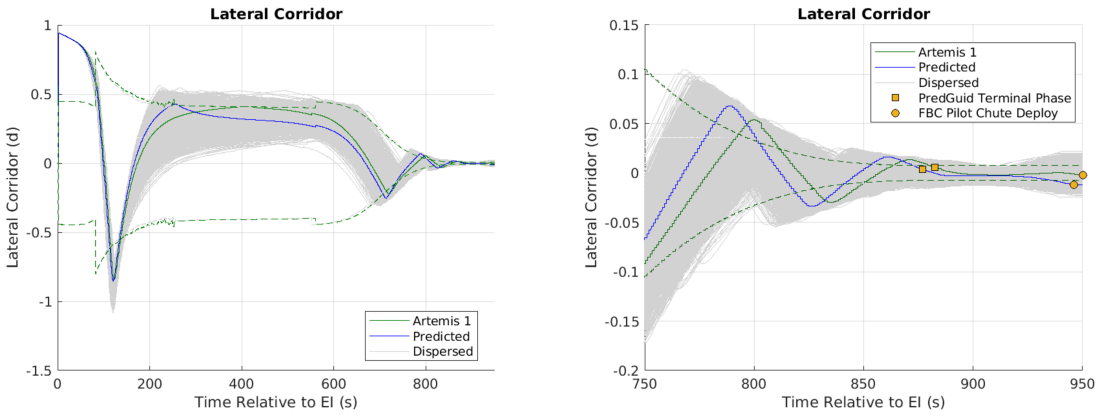

(a) Artemis I Lateral Corridor (Entire Atmospheric Entry)

(b) Artemis I Lateral Corridor (Near End of Guided Flight)

Figure 9: Artemis I Lateral Corridor

Guidance Results

The Artemis I flight did not skip as high as predicted. The geodetic altitude at skip apogee was 287.4 kft for the actual flight while the predicted was 293.5 kft. This is likely due to a less dense atmosphere during the first pass and slightly less lift-to-drag (L/D) than predicted. However, the phase transition times compare very well between the Artemis I flight and the best simulated prediction.

Figure 10(a) shows the geodetic altitude versus range-to-go with call-outs for the 1st and 2nd max gloads, skip apogee, and key chute deploy epochs. Figure 10(b) shows the geodetic altitude versus time relative to EI. Figure 11(a) shows the sensed acceleration magnitude versus time relative to EI. These figures show a successful skip entry.

Figure 11(b) shows the ground track near the landing site. The initiation of the Terminal phase is shown as a square. Both the actual flight and predicted trajectories initiate the Terminal phase at roughly the same coordinates within 2.7 nmi of the landing target. The circles show the FBC pilot chute deploy points which mark the end of guided entry flight. The landing target is shown as a cross. The drift under the chutes due to wind is obvious. Table 4 gives the miss distance and coordinates of drogue deploy, main deploy, and splashdown. Orion is required to land within 5.4 nmi of the landing target, and this requirement was met.

Figure 12(a) shows the actual and commanded bank angles versus time relative to EI. Note that the bank angle tracks the commanded bank angle very well until about the last 90 seconds of guided flight. Figure 12(b) shows the bank angles zoomed in to the last 90 seconds of the guided flight. Figure 12(b) also shows the bank angle if no wind were encountered. The bank angle from the navigation system assumes no wind. As the vehicle slows down, the wind speed becomes significant relative to the speed of the vehicle. At this point, the assumption to ignore wind in the on-board computation of bank angle breaks down. This may be a contributing factor to the miss distance at drogue deploy. However, without an on-board method of determining wind speed, there is not much that can be done about this.

Density and L/D Estimator Performance The PredGuid entry guidance uses the measured acceleration to estimate an atmospheric density scale factor (Dens_Fact_Filt) and the actual L/D of the vehicle (Lod_Est_Filt). The value of Dens_Fact_Filt is applied to the on-board 1976 standard atmosphere model in the NPC to account for higher or lower density. A value of 1 indicates that the on-board model is used with no scaling. The value of Lod_Est_Filt is used directly in the NPC as the hypersonic L/D. At the initiation of the Ballistic phase, a snapshot of the value of Lod_Est_Filt is taken and stored in the variable Lod_Est_Filt_Ballistic. This constant value of L/D is then used throughout the Ballistic phase. The estimators are active after the Initial Roll phase when the drag acceleration is above the parameter D_Estimators (1.6 ft/s2). While these parameters are computed for much of the trajectory, they are only used during the Up Control and Ballistic phases.

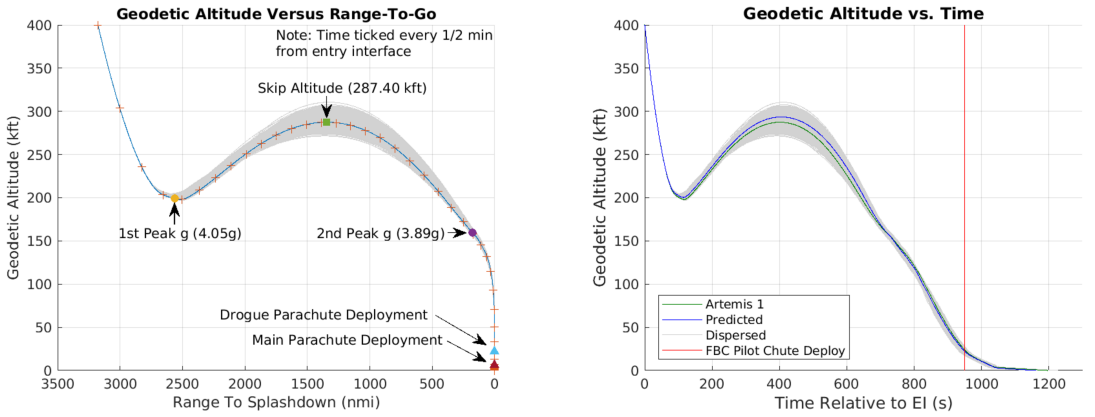

(a) Artemis I Geodetic Altitude vs. Range-To-Go

(b) Artemis I Geodetic Altitude vs. Time Relative to EI

Figure 10: Artemis I Geodetic Altitude vs. Range-To-Go and Time

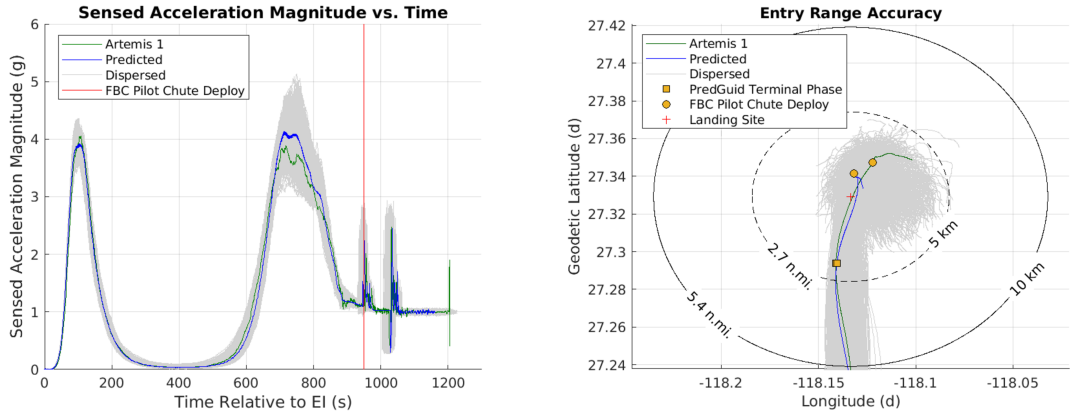

(a) Artemis I Sensed Acceleration vs. Time Relative to EI

(b) Artemis I Landing Accuracy

Figure 11: Artemis I Performance Plots

Table 4: Miss Distance and Coordinates of Chute Deploys and Splashdown

Parameter	Miss Distance (nmi)	Geodetic Altitude (ft)	Geodetic Latitude (d)	Longitude (d)
Drogue deployed	1	22273.99	27.34817	-118.12188
Main deployed	1	6352.48	27.35166	-118.11144
Splashdown	2	0	27.34852	-118.10181

Figure 13(a) shows the value of Dens_Fact_Filt. Figure 13(b) shows a composite of Lod_Est_Filt_Ballistic during the Ballistic phase, and Lod_Est_Filt during the other phases. According to the PredGuid estimators, the Artemis I flight encountered roughly a 10% less dense atmosphere than the 1976 standard atmosphere. It also had roughly 5% less L/D than predicted. This is the most likely cause of the differences in the guidance solutions observed during each PredGuid phase. The small differences observed in the earliest phases waterfall into larger differences in the later phases.

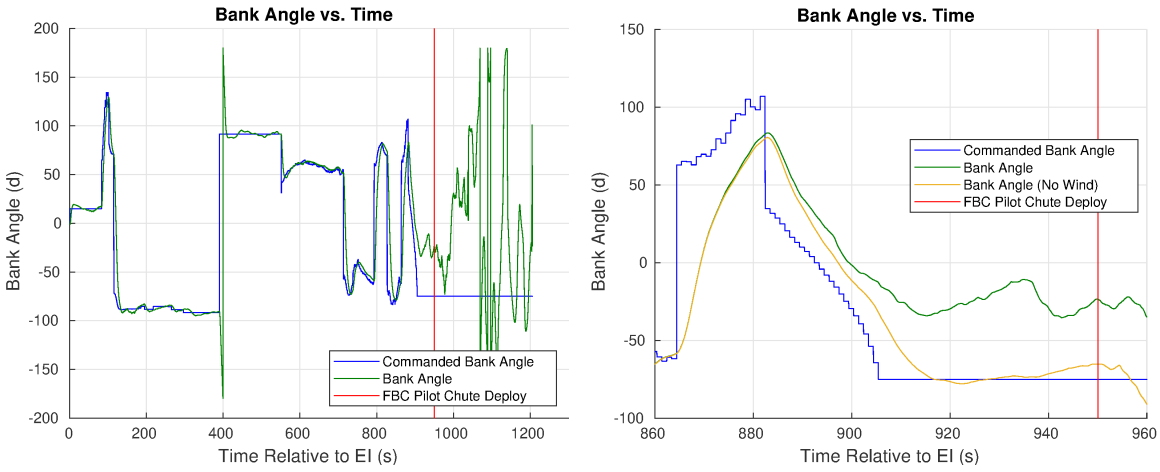

(a) Whole Atmospheric Entry

(b) Last 90 sec of Guided Flight

Figure 12: Artemis I Bank Angle vs. Time Relative to EI

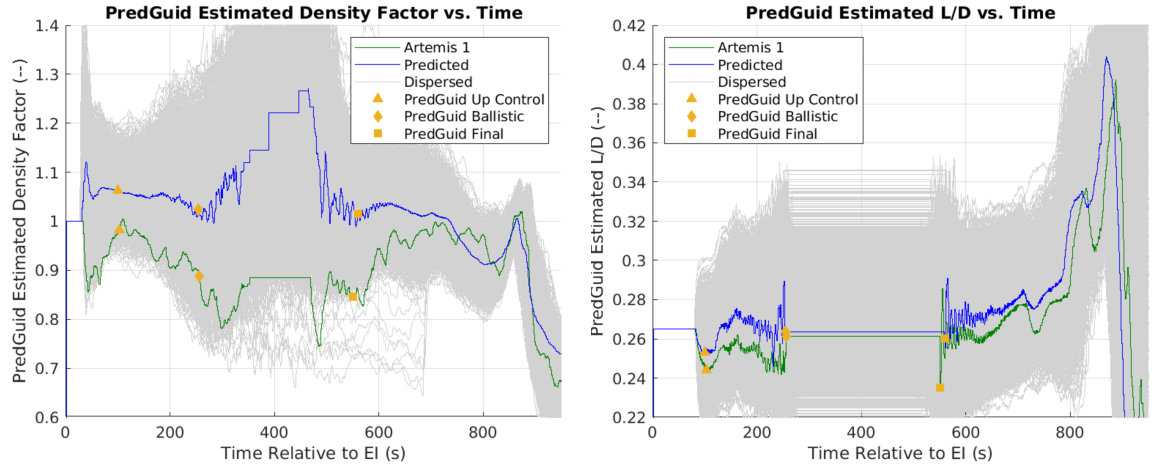

(a) Artemis I PredGuid Filtered Density Estimate Factor (Dens_Fact_Filt)

(b) Artemis I PredGuid Filtered L/D Estimate (Lod_Est_Filt)

Figure 13: Artemis I PredGuid Filtered Estimates

Bank Angle Rate Performance Figure 14 shows the bank angle rate versus time relative to EI. As expected, the bank angle rates reach +-15 deg/s during the bank reversals. Other smaller bank maneuvers reach around +-10 deg/s, which is also as expected.

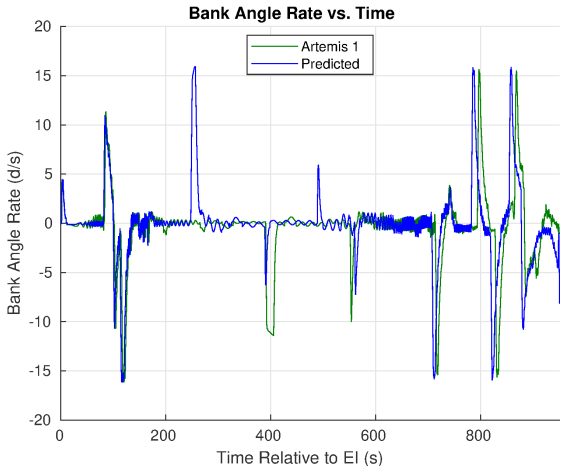

Figure 14: Artemis I Bank Angle Rate vs. Time

Performance at Transition to Final Phase The state at the transition to Final phase is an important measure of the guidance performance. Recall that EI is defined at an altitude of 400 kft. However, for skip entries such as Artemis I, the transition to Final phase is effectively at the second atmospheric entry since this is the point where the drag acceleration begins to increase.

Each figure in this section shows data at the transition to Final phase. The gray dots are the spread from the entry monte carlo made on Flight Day 23 (FD23) at a time of 72 hours before EI. The green circle is the Artemis I flight data. The blue square corresponds to the best simulated prediction used for other comparisons in this document.

Figure 15(a) shows the geodetic altitude versus range-to-target. As noted earlier, the Artemis I flight did not skip as high as predicted, and this shows at the transition to Final phase. While the geodetic altitude is within the range of outliers in the FD23 dispersed data, it is an outlier itself. The range-to-target is within the FD23 prediction.

Figure 15(b) shows the geodetic latitude versus longitude. Figure 15(c) shows the drag acceleration (D_Mag) versus speed (V_Mag). Figure 15(d) shows the altitude rate (Alt_Rate) versus speed (V_Mag). In all figures, the Artemis I flight data is within the predicted dispersion limits.

Performance at Forward Bay Cover Pilot Chute Deploy The goal of the entry guidance is to deliver the vehicle to the desired target location at FBC pilot chute deploy. Each figure in this section shows data at the FBC pilot chute deploy. The gray dots are the spread from the entry monte carlo made on Flight Day 23 (FD23) at a time of 72 hours before EI. The green circle is the Artemis I flight data. The blue square corresponds to the best simulated prediction used for other comparisons in this document.

Figure 16(a) shows the geodetic altitude versus range-to-target. Figure 16(b) shows the geodetic latitude versus longitude. The Artemis I flight data is within the predicted dispersion limits.

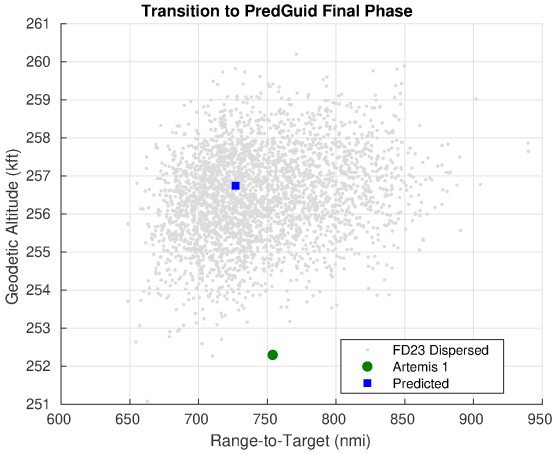

(a) Geodetic Altitude vs. Range-To-Target

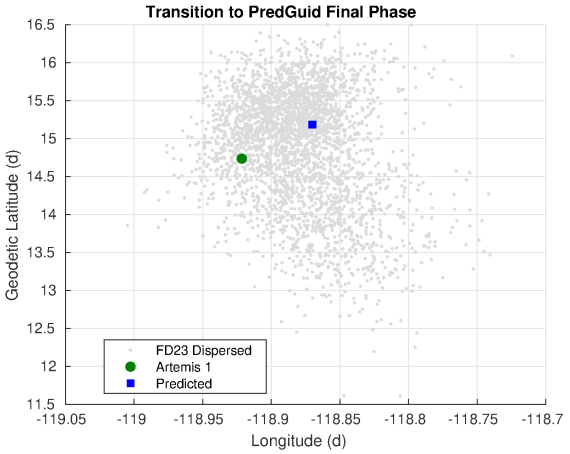

(b) Geodetic Latitude vs. Longitude

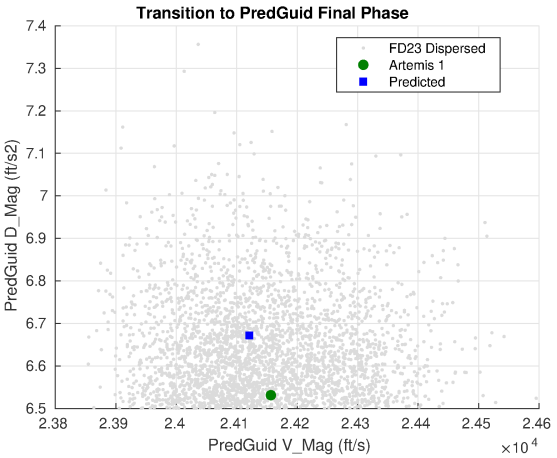

(c) PredGuid D_Mag vs. V_Mag

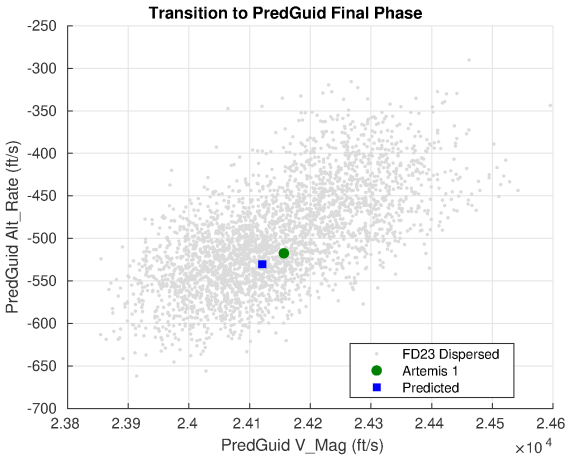

(d) PredGuid Alt_Rate vs. V_Mag

Figure 15: Transition to Final Phase Metrics

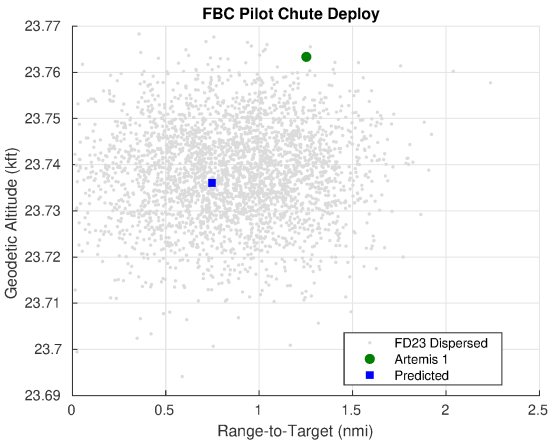

(a) FBC Pilot Chute Deploy: Geodetic Altitude vs. Range-To-Target

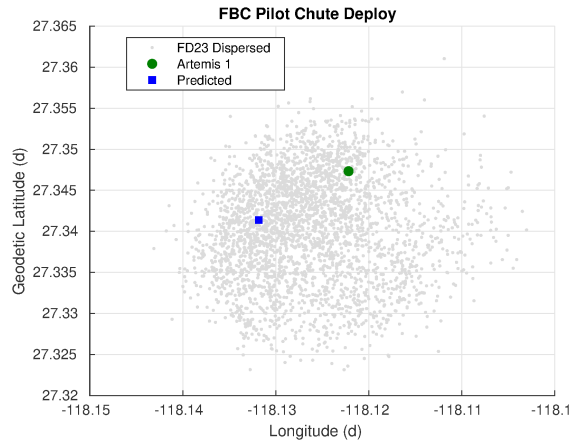

(b) FBC Pilot Chute Deploy: Geodetic Latitude vs. Longitude

Figure 16: FBC Pilot Chute Deploy Metrics

ENTRY CONTROL

Crew Module Reaction Control System

Orion Entry Control utilizes the Crew Module (CM) Reaction Control System (RCS) thrusters to produce torque on the vehicle and achieve attitude control commands. CM RCS consists of two fully-redundant strings of thrusters with six thrusters on each string. Each thruster in the string is mounted such that it produces a nearly pure positive or negative torque about a primary body axis. Table 5 provides the nomenclature for labeling the twelve CM RCS jets. Figure 17 shows where each thruster is located on the crew module.

Table 5: Crew Module CM RCS Thruster Labeling Nomenclature

String A	String B	Function
CRR-A	CRR-B	CM Roll Right
CRL-A	CRL-B	CM Roll Left
CPU-A	CPU-B	CM Pitch Up
CPD-A	CPD-B	CM Pitch Down
CYR-A	CYR-B	CM Yaw Right
CYL-A	CYL-B	CM Yaw Left

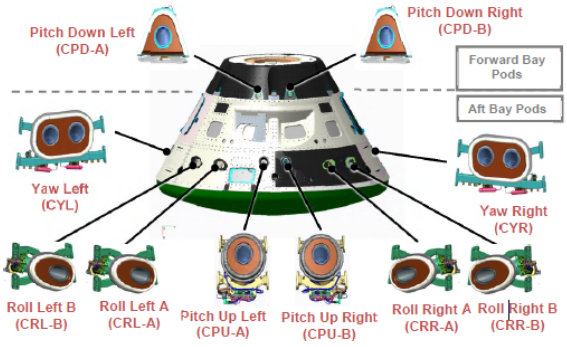

Figure 17: CM RCS Location and Nomenclature

Entry Control Design and Methodology

The CM control system (CNC) is a digital controller that operates at a 40-Hz rate on the Flight Computer Module (FCM) within the Guidance, Navigation, Control, and Propulsion (GNCP) partition. The block diagram for attitude control during Entry operation is shown in Figure 18.

Entry guidance provides the commanded freestream attitude and attitude rates. The controller first subtracts the navigated freestream attitude from the guidance command to produce the freestream attitude error. Afterwards the bank angle error is modified to have a sign in the direction resulting in the shortest maneuver time to the commanded bank angle and the angle of attack and angle of sideslip errors are phase-wrapped to result in the minimum angle distance. The direction of shortest time is determined by estimating the time to perform a rate limited maneuver by continuing in the direction of the initial bank rate and comparing against the time to maneuver in the opposite direction. The modified attitude error is then multiplied by the control gains and constrained to a maximum magnitude to produce the control freestream rate command. The freestream rate command is transformed to produce body rate commands that are used by the rate controller to produce bi-level CM RCS jet commands. The jet commands are used by downstream thruster logic to produce CM RCS thruster on-times that meet system constraints such as per-thruster minimum on time and minimum off time, as well as the number of simultaneous thrusters allowed to fire or shut down per cycle.

The Entry phase of flight is the period between EI and deployment of the drogue parachutes. During the Entry phase of flight the control system is requried to maintain heatshield forward and perform bank angle tracking to steer the vehicle towards the landing site. Attitude and attitude rate commands are produced by the Entry Guidance (GDE) domain and the CM Control domain (CNS) is responsible for generating CM RCS thruster commands.

During the Entry phase of flight the vehicle experiences exo-atmospheric and atmospheric flight conditions. Exo-atmospheric conditions occur between EI and when the vehicle first enters sensible atmosphere (first entry) and also from when the vehicle exits atmosphere during skip guidance and re-entry into the atmosphere (second entry). During exo-atmospheric portions of flight the control system performs 3-axis attitude control. The large dynamic pressures during atmospheric flight produce aerodynamic torques that mostly stabilize the vehicle about a trim condition but become destabilizing in the subsonic region of flight. Inside the atmosphere, Entry control is used to augment stability with three-axis attitude rate damping and to perform

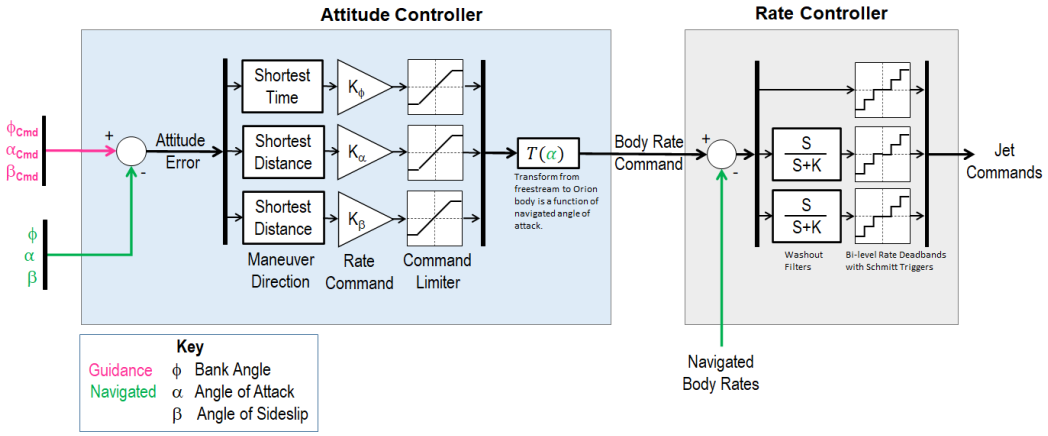

Figure 18: Orion Entry Control Block Diagram

attitude maneuvering that is limited to rotations about the bank axis to steer the vehicle towards the landing target. The Entry controller is gain scheduled based on both acceleration and velocity. The exo-atmospheric gains are constant, while atmospheric gains are scheduled on velocity. Transition between exo-atmospheric and atmospheric gains is achieved using a sensed acceleration schedule. The atmospheric gains are tailored for hypersonic, supersonic, transonic, and subsonic phases of flight.

Aerothermal Detailed Test Objective Unique to the Artemis I mission was the inclusion of the CM Aerothermal Detailed Test Objective (ADTO). The ADTO was a series of open-loop commands executed during hypersonic atmospheric flight. Temperature sensors were included on the CM backshell and used to measure aerothermal heating to observe the impacts that thruster firings have on backshell heating, this data has been used to validate Orion aerothermal models. Each planned thruster firing is preceded by a quiet period where no thrusters are fired. Following the open loop firing, active flight control corrects any resulting disturbance. The ADTO can be suspended by bank reversals, significant attitude or rate disturbances, and detected thruster faults. Logic to support the ADTO has been removed from Entry flight software for Artemis II+ missions.

Control Results

Figure 19 shows the commanded bank angle versus the navigated bank angle and highlights the bank reversals. CM control was able to successfully track the commanded bank during entry.

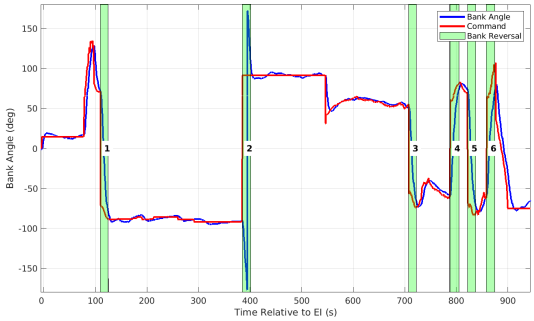

Figure 19: Bank Tracking

Figure 20(a) shows the control rate errors with respect to the changing deadbands during Entry guidance and control. The region the ADTO was active is shaded in blue in Figure 20(a). Large error spikes in the roll

channel (p) indicate when the guidance command changed and a maneuver was performed. It can be seen that the CM instability in the subsonic region resulted in more CM RCS firings in the pitch and yaw axes, otherwise the firings were primarily limited to the CM roll axis and occurred during attitude maneuvers.

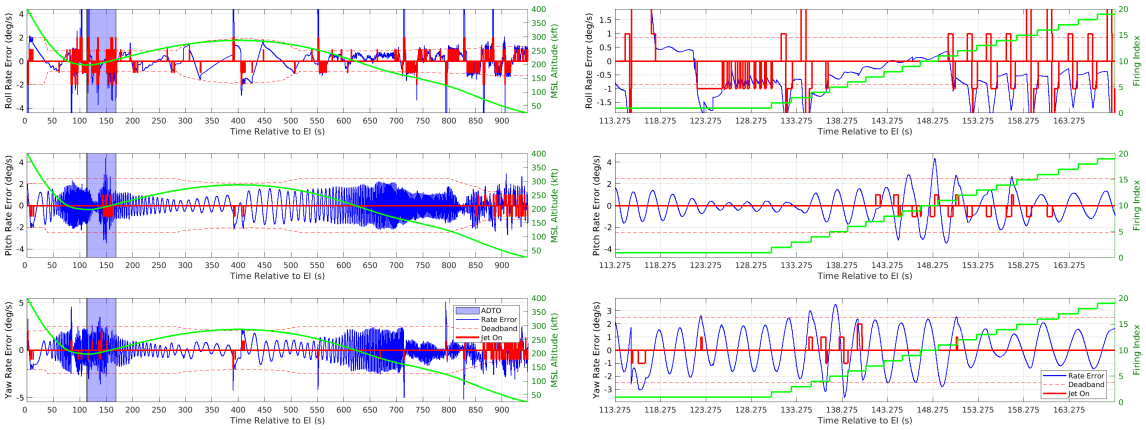

(a) Body Rate Error During Entry

(b) Body Rate Error During the CM Aerothermal DTO

Figure 20: Body Rate Error

Entry attitude control can be visualized in phase plane space with an effective attitude deadband computed by dividing the average attitude gain by the average rate deadband during the attitude maneuver. Figure 21 shows the phase planes during each bank reversal. It can be seen that control was well behaved during the bank reversals and that all reversals were in the direction of minimum-distance; this is expected as all reversals had a near-zero initial bank rate.

Aerothermal Detailed Test Objective Figure 20(b) is focused on the ADTO region shown in Figure 20(a). It can be seen that the ADTO start time was delayed due to a bank maneuver but afterwards was able to complete without any further interruption. The open loop firings cause small excursions outside of the control rate deadbands; however, the CM is stable during the hypersonic region and the CM state quickly returns to within control deadbands after the firing completes.

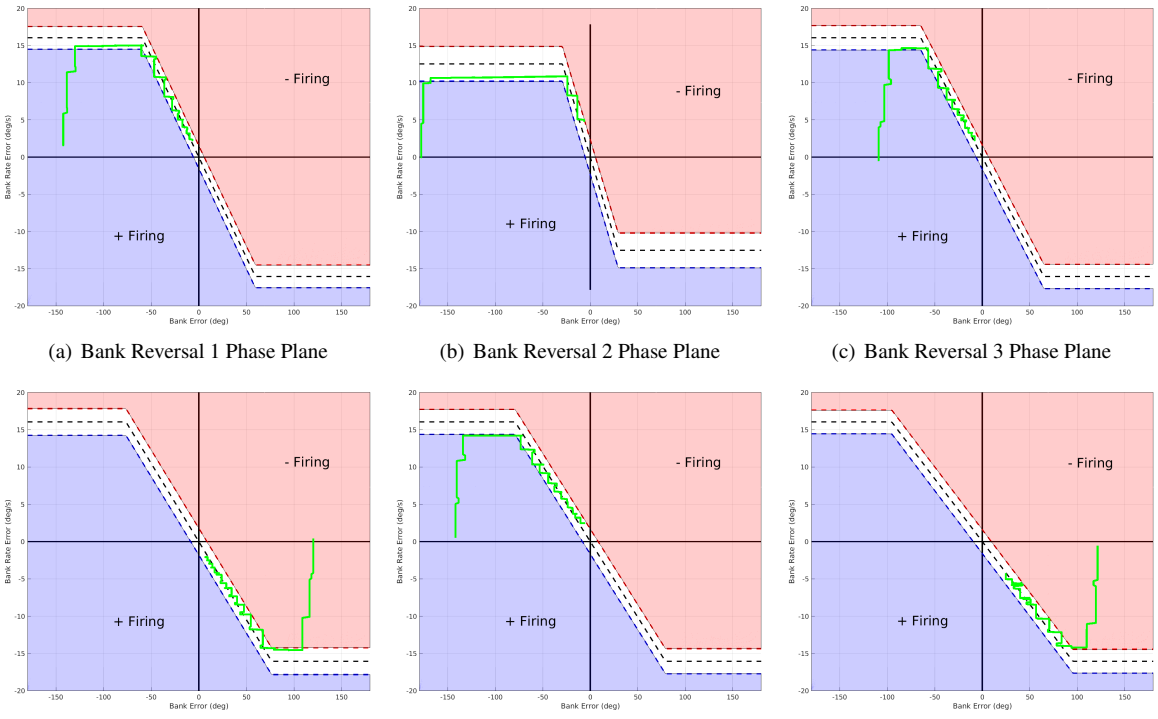

(a) Bank Reversal 1 Phase Plane (b) Bank Reversal 2 Phase Plane (c) Bank Reversal 3 Phase Plane

(d) Bank Reversal 4 Phase Plane (e) Bank Reversal 5 Phase Plane (f) Bank Reversal 6 Phase Plane

Figure 21: Bank Reversal Phase Plane

CONCLUSION

Artemis I is the first successful demonstration of a skip entry for a human rated vehicle. Differences between the actual and predicted flight are likely due to a 10% less dense atmosphere and a 5% less L/D from the preflight predictions. However, these values were well within the allowable dispersion ranges. The main impact was a lower than predicted skip apogee and a shift in the timing of the bank reversals. Even with these differences, the entry GNC system performed very close to the predicted flight.

ACKNOWLEDGMENT

The authors would like to recognize the technical achievements of the original Apollo engineers. For their significant contributions to the success of the Artemis I entry, the authors would like to acknowledge the support of former Orion Entry MODE Team members Timothy J. Crull, Michael A. Tigges, Gregg H. Barton, Zachary R. Putnam, Andrew Barth, and Travis J. Bailey. The authors would also like to thank their families for their support.

NOTATION

$\frac{L}{D}$	Lift-over-Drag Ratio of Vehicle
γ	Inertial Topocentric Flight Path Angle
α	Angle of attack, deg
β	Angle of sideslip, deg
ϕ	Bank Angle, deg

REFERENCES

[1] "View the Best Images from NASA's Artemis I Mission", NASA, 29 Sept. 2023, www.nasa.gov/humans-in-space/view-the-best-images-from-nasas-artemis-i-mission/.

[2] Putnam, Z. R., & Rea, J. R., "A Comparison of Two Skip Entry Guidance Algorithms," AIAA-2007-6424, August 2007.

[3] Putnam, Z. R., & Neave M. D., & Barton G. H., "PredGuid Entry Guidance for Orion Return from Low Earth Orbit," IEEE Aerospace Conference, No. 05447010, 2010.

[4] Bairstow, S. H., "Reentry Guidance with Extended Range Capability for Low L/D Spacecraft," S. M. Thesis, Department of Aeronautics and Astronautics, Massachusetts Institute of Technology, February 2006

[5] Bairstow, S. H, & Barton, G., "Orion Reentry Guidance with Extended Range Capability Using PredGuid," AIAA-2007-6427, August 2007.

[6] Morth, R., "Reentry Guidance for Apollo," MIT/IL R-532 Vol. I, 1966.

[7] Rea, J. R., "Orion Exploration Mission Entry Interface Target Line," AAS/AIAA Space Flight Mechanics Meeting, AAS Paper Number 16-485, Napa, California, February 14 - February 18 2016.

[8] Gutkowski, J., & Dawn, T., & Williams, J., "DRO Mission Overview", September 2013.

[9] McNamara, L. W., "Definition Of The Design Entry Trajectory and Entry Flight Corridor For The NASA Orion Exploration Mission 1 Using An Integrated Approach And Optimization", AAS Guidance, Navigation and Control Conference, AAS Paper Number 14-094, Breckenridge, Colorado, January 31 - February 5 2014.

[10] Gamble, J. D., C. J. Cerimele, T. E. Moore, and J. Higgins. "Atmospheric Guidance Concepts for an Aeroassist Flight Experiment." Journal of the Astronautical Sciences 36, 1988: 45-71.